Article

Cell Reports

Information Coding through Adaptive Gating of Synchronized Thalamic Bursting

Graphical Abstract

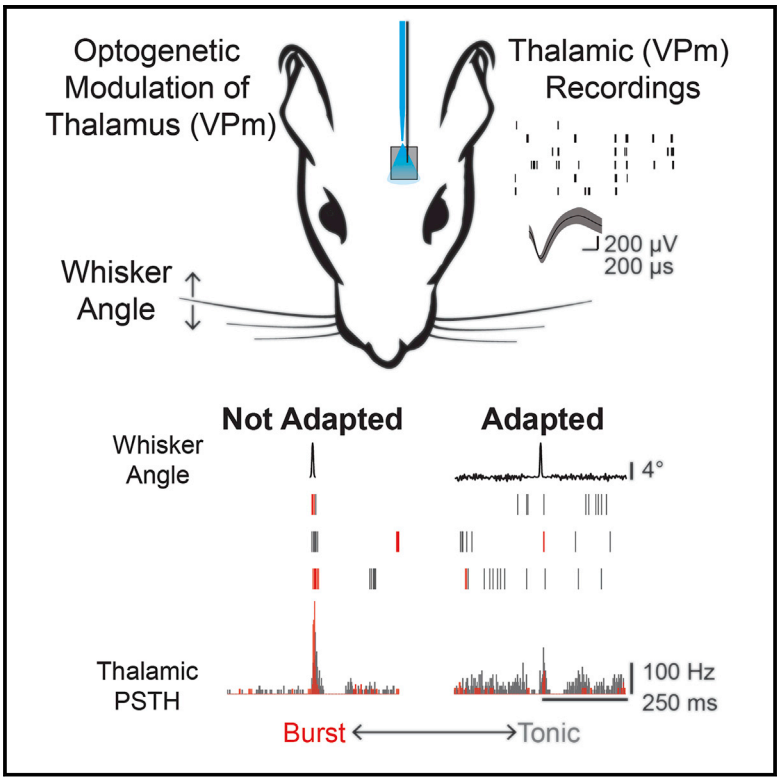

Authors

Clarissa J. Whitmire, Christian Waiblinger, Cornelius Schwarz, Garrett B. Stanley

Correspondence

garrett.stanley@bme.gatech.edu

In Brief

Whitmire et al. show that sensory adaptation dynamically modulates feature-driven synchronized bursting along a continuum in thalamocortical projection neurons. This shift in encoding may serve as a potential mechanism to facilitate context-dependent information processing.

Highlights

- Bottom-up adaptation continuously modulates thalamic burst/tonic firing
- Adaptation modulates the degree of stimulus-evoked synchronized bursting
- Adapting stimuli shift thalamic encoding from detection to discrimination mode
- Proposed adaptive mechanism of action is sustained depolarization of thalamic neurons

Whitmire et al., 2016, Cell Reports *14*, 1–13
February 2, 2016
http://dx.doi.org/10.1016/j.celrep.2015.12.068

CellPress

Please cite this article in press as: Whitmire et al., Information Coding through Adaptive Gating of Synchronized Thalamic Bursting, Cell Reports (2016), http://dx.doi.org/10.1016/j.celrep.2015.12.068

Cell Reports
Article

Information Coding through Adaptive Gating of Synchronized Thalamic Bursting

Clarissa J. Whitmire,[1] Christian Waiblinger,[1,2,3] Cornelius Schwarz,[2,3] and Garrett B. Stanley[1,*]
[1]Wallace H. Coulter Department of Biomedical Engineering, Georgia Institute of Technology and Emory University, Atlanta, GA 30332, USA
[2]Systems Neurophysiology, Werner Reichardt Centre for Integrative Neuroscience, University of Tübingen, Tübingen 72074, Germany
[3]Department of Cognitive Neurology, Hertie Institute for Clinical Brain Research, University of Tübingen, Tübingen 72074, Germany
*Correspondence: garrett.stanley@bme.gatech.edu
http://dx.doi.org/10.1016/j.celrep.2015.12.068

SUMMARY

It has been posited that the regulation of burst/tonic firing in the thalamus could function as a mechanism for controlling not only how much but what kind of information is conveyed to downstream cortical targets. Yet how this gating mechanism is adaptively modulated on fast timescales by ongoing sensory inputs in rich sensory environments remains unknown. Using single-unit recordings in the rat vibrissa thalamus (VPm), we found that the degree of bottom-up adaptation modulated thalamic burst/tonic firing as well as the synchronization of bursting across the thalamic population along a continuum for which the extremes facilitate detection or discrimination of sensory inputs. Optogenetic control of baseline membrane potential in thalamus further suggests that this regulation may result from an interplay between adaptive changes in thalamic membrane potential and synaptic drive from inputs to thalamus, setting the stage for an intricate control strategy upon which cortical computation is built.

INTRODUCTION

The majority of our sensations travel from the periphery through the thalamus before reaching cortex, such that each sensory region of thalamus has a corresponding cortical projection. Despite the strategic positioning of this brain structure, surprisingly little is known about its ultimate function. Whereas it is clear that the various nuclei of the thalamus play a vital role in high-level functions such as attention, perception, and consciousness, as evidenced by lesioning of the thalamus (Schmahmann, 2003; Van der Werf et al., 2000), it is unclear as to what active role it plays. Due to a preponderance of T-type calcium channels in this region, thalamic neurons are particularly prone to vacillate between burst and tonic firing modes in a state-dependent manner (Suzuki and Rogawski, 1989). Although thalamic bursting was originally associated with a disconnection between the cortex and the periphery (Steriade et al., 1993), it has been posited that regulation of burst firing in the thalamus may serve as a dynamic gating mechanism for controlling information flow to cortex (Crick, 1984; Lesica and Stanley, 2004; Lesica et al., 2006; Sherman, 1996; Wang et al., 2007). It has been established that the continuous transition between burst and tonic firing is determined by both the subthreshold membrane potential of the neuron as well as the ongoing synaptic activity (Mukherjee and Kaplan, 1995; Wolfart et al., 2005). However, what is not at all understood is how the transition between burst and tonic firing modes is modulated in a dynamic sensory environment, how this is coordinated across the neuronal population, and how this thalamic state transition affects information transmission.

The rapid adaptation of functional properties in response to changes in sensory stimulation, over a range of temporal and spatial scales, is common to all sensory modalities (Wark et al., 2007). For example, a simple change in statistics of a sensory signal, such as the stimulus contrast, can lead to a cascade of changes in sensory encoding, from gain rescaling (Fairhall et al., 2001; Shapley and Victor, 1979) to fundamental alterations to the feature selectivity of sensory neurons (Lesica et al., 2007), which are even more pronounced when considering differential adaptation across neuronal populations. This has led to the proposal that this form of adaptation serves to enhance information transmission in the dynamic sensory environments (Sharpee et al., 2006). In the thalamocortical pathway, the functional role of adaptation in modulating the spike timing of sensory-evoked activity within and across thalamic neurons has a particularly strong impact on the activation of their downstream cortical targets that rely on weak but highly convergent inputs from the thalamus (Bruno and Sakmann, 2006). We have recently shown that adaptation serves to desynchronize the firing activity of thalamic neurons (Ollerenshaw et al., 2014; Wang et al., 2010), but the interaction between adaptive mechanisms and the regulation of synchronized bursting across thalamic inputs to cortex is not at all understood yet could serve as a robust mechanism for gating information flow as a function of bottom-up and top-down influences.

Here, we demonstrate a direct link between ongoing bottom-up sensory adaptation and the modulation of feature-evoked bursting in the ventral posterior medial (VPm) region of the thalamus in the vibrissa pathway of the rat. Baseline recordings were obtained under fentanyl anesthesia, corresponding to a relatively hyperpolarized thalamic state, such that adaptation transitioned the thalamus from a burst to a tonic firing mode. Using optogenetic depolarization to directly modulate thalamus, we identified

Please cite this article in press as: Whitmire et al., Information Coding through Adaptive Gating of Synchronized Thalamic Bursting, Cell Reports (2016), http://dx.doi.org/10.1016/j.celrep.2015.12.068

a graded, sustained depolarization of thalamic neurons as the likely mechanism by which adapting stimuli modulate evoked bursting activity, working in concert with changes in synaptic drive, to gate thalamic activity. From the perspective of timing-based ideal observer analysis of thalamic spiking activity, sensory adaptation led to reduced detectability but enhanced discriminability at an intermediate level of adaptation. Furthermore, paired recordings demonstrated a reduction in not only synchronous firing but synchronous burst firing with more profound adaptation. Therefore, the regulation of stimulus-driven synchronized bursting may be a critical mechanism for gating peripheral inputs that form sensory cortical representations.

RESULTS

Adaptation Shifts Thalamus from Burst to Tonic Firing

We recorded single-unit activity in the VPm nucleus of the rat vibrissal lemniscal pathway in response to single-whisker stimuli with or without optogenetic modulation of the thalamic membrane potential under fentanyl-cocktail anesthesia (Figure 1A). The sensory stimulus consisted of an ethologically relevant feature embedded in an ongoing adapting background stimulus (Figure 1B; whisker angle; see Experimental Procedures). The shape of the feature was designed to mimic high-velocity deflections, or stick-slip events, that match the feature selectivity of thalamic neurons in this pathway (Petersen et al., 2008; Ritt et al., 2008; Wolfe et al., 2008), whereas the amplitudes of the feature were chosen to span the behavioral range of feature detectability from ongoing sensory stimulation (Stüttgen et al., 2006; A_F = 0°, 1°, 2°, 4°, 8°, and 16°; rise time = 5 ms). The frequency content of the adapting noise stimulus spanned 0–200 Hz to sample relevant whisker stimulation frequencies (Lottem and Azouz, 2008) within the physical limitations of the whisker stimulator, whereas the amplitude of the noise was set at levels perceptible to the animal (A_N = 0°, 0.07°, 0.17°, 0.34°, 0.68°, 2.75°, and 5.5°), as ascertained in a separate study (Waiblinger et al., 2015a). Note that we have demonstrated that this form of rapid adaptation is very similar in the presence of repetitive/periodic whisker stimulation and "white noise" stimulation, depending primarily on the overall power in the adapting stimulus (Zheng et al., 2015) and is distinctly different from forms of stimulus-specific adaptation. Whereas sensory adaptation has many definitions/meanings within specific sensory modalities, the universal ability of the pathway to adapt to ongoing changes in the stimulus statistics has been demonstrated in auditory (Dean et al., 2005), visual (Fairhall et al., 2001), and somatosensory (Maravall et al., 2007) pathways. Here, the statistics of the adapting stimulus were systematically varied to investigate the changes in feature selectivity in the presence of varying statistical properties of the adapting stimulus.

Thalamic neurons responded strongly when stimulus features were presented in isolation (not adapted condition), but the stimulus feature elicited fewer spikes when surrounded by an adapting noise stimulus (adapted condition), even when the amplitude of the adaptive noise stimulus was relatively small compared to the amplitude of the feature (shown for an example neuron in Figure 1B; A_F = 8°; A_N = 0.32°). In this example neuron, the not adapted feature response was strong (as defined by the number of elicited spikes) and temporally precise (as defined by the first spike latency jitter) on nearly every trial (Figure 1B; not adapted). In contrast, the adapted neural response for this example neuron showed greater background firing due to the evoked response from the adapting stimulation and reduced feature-evoked activity (Figure 1B; adapted). Across cells, the background firing activity due to the evoked response from the adapting stimulus was increased relative to the spontaneous firing in the not adapted condition ($p = 1.18e-5$; paired Wilcoxon signed-rank test; data not shown). The response to the stimulus feature (R_F), defined as the number of spikes in a 10-ms window following feature presentation (see Supplemental Experimental Procedures), increased with increasing feature amplitude across cells (Figure 1C, solid; not adapted; n = 26 cells) but was significantly attenuated in the adapted condition (Figure 1C, dashed; adapted; n = 26 cells; $^*p < 0.05$; paired Wilcoxon signed-rank test with Bonferroni-Holm correction). The first spike latency (FSL) in response to the features in the not adapted condition was consistent with the latencies expected for VPm neurons (A_F = 16°; FSL = 5.7 ± 0.7 ms; n = 26 cells). As expected for sensory adaptation, the FSL increased in the adapted condition (A_F = 16°; FSL = 8.2 ± 0.8 ms; n = 26 cells; $p = 3.67e-5$; paired Wilcoxon signed-rank test). Note that the degree of adaptation observed in these thalamic neurons was consistent with that observed for more-simple, periodic whisker stimulation (Temereanca et al., 2008; Wang et al., 2010) and that the amplitude of the increased latency with adaptation was consistent with VPm neurons as opposed to neurons located in the nearby posteromedial (POm) complex of the thalamus (Ahissar et al., 2000). The FSL jitter, a metric of temporal precision, was also higher in the adapted condition than in the not adapted condition (Figure 1D; n = 26 cells; $^*p < 0.05$; paired Wilcoxon signed-rank test with Bonferroni-Holm correction).

Shifts in thalamic state are known to induce shifts in firing modes, specifically in the context of burst and tonic firing (Sherman, 2001). What is not well understood is how adaptation changes thalamic state and, in turn, modulates tonic and burst firing. To isolate bursts likely originating from T-type calcium channels, burst spikes were defined as two or more spikes with an inter-spike interval (t_{isi}) of less than 4 ms with the first spike in the burst preceded by silence ($t_{silence}$) of 100 ms or more (Figure 1E), consistent with classical definitions (Lesica et al., 2006; Lu et al., 1992; Reinagel et al., 1999). Burst and tonic spikes are color coded for a typical thalamic neuron in Figure 1B (red and gray, respectively). In addition to the reduction in the feature-evoked spiking activity, this example neuron displays a disproportionate loss of burst spikes in the adapted condition (Figure 1B). Consistent with this example neuron, the presence of the adapting noise stimulus led to a decrease in the total number of feature-evoked spikes across cells (Figure 1C; n = 26 cells) but an even larger reduction in the number of burst spikes in response to the feature as captured by the burst ratio, defined as the number of burst spikes in the feature response window divided by the total number of spikes in the feature response window (Figure 1G; n = 26 cells; $p = 2.63e-5$; Wilcoxon signed-rank test).

Furthermore, a limited number of single-unit recordings were performed in the awake behaving, head-fixed rat in a similar

Please cite this article in press as: Whitmire et al., Information Coding through Adaptive Gating of Synchronized Thalamic Bursting, Cell Reports (2016), http://dx.doi.org/10.1016/j.celrep.2015.12.068

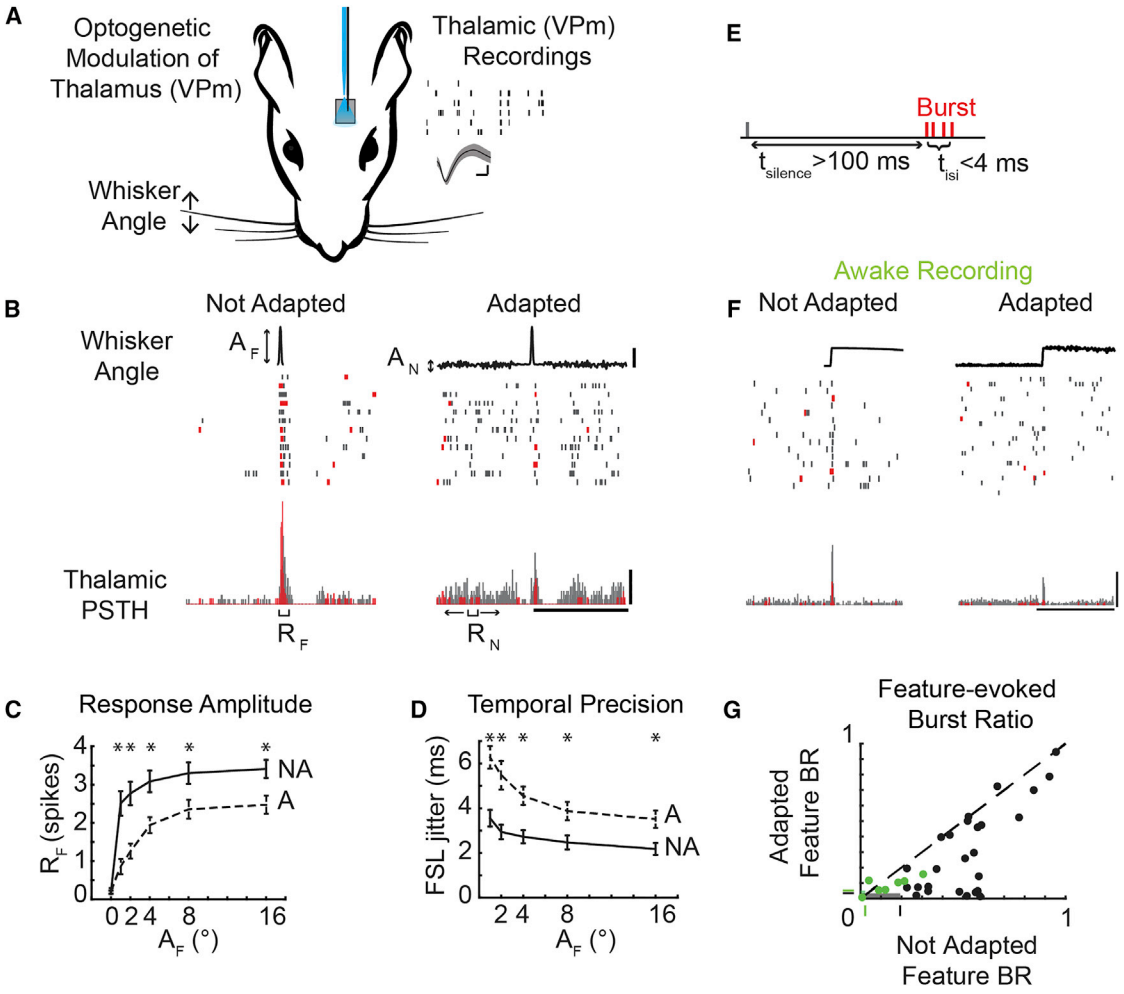

Figure 1. Sensory Adaptation Modulates Burst/Tonic Firing

(A) Extracellular recordings from the ventral posteromedial (VPm) nucleus of the thalamus during sensory stimulation and, in a subset of animals transfected with channelrhodopsin, light modulation applied via an optic fiber. Waveform scale bars represent 200 μV and 200 μs.

(B) Example neural response to a sensory feature (A_F = 8°) presented in isolation (A_N = 0°) and with adaptation (A_N = 0.168°; 125°/s) with burst spikes colored red and tonic spikes colored gray. A_F, amplitude of stick-slip feature (°); A_N, SD of adapting noise (°); R_F, feature-evoked response; R_N, adapting noise-evoked response. The scale bars represent 4°, 250 ms, and 100 Hz.

(C) Mean evoked response to not adapted features responses (black; A_N = 0°) and adapted feature responses (gray; A_N: 0.168°) across cells (n = 26 cells; mean ± SEM; *p < 0.05; paired Wilcoxon signed-rank test with Bonferroni-Holm correction NA, not adapted; A, adapted).

(D) First spike latency jitter in response to adapted features (gray) and not adapted features (black; n = 26 cells; mean ± SEM; *p < 0.05; paired Wilcoxon signed-rank test with Bonferroni-Holm correction).

(E) A burst is defined as two or more spikes with an interspike interval of 4 ms or less (t_{isi}) with the first spike preceded by at least 100 ms of silence ($t_{silence}$).

(F) Example neuron recording from the awake behaving animal in response to sensory features with and without noise (A_F = 9°; A_N = 0.48°). The scale bars represent 4°, 100 Hz, and 250 ms.

(G) Feature burst ratio in adapted and not adapted condition across cells (n = 33 cells [26 cells from anesthetized preparation, black; seven cells from awake preparation, green]; p = 4.99e − 6; paired Wilcoxon signed-rank test).

adaptation paradigm (n = 7 cells, 2 rats). Although the embedded feature was different in detail from that used in the anesthetized recordings, the rise time and feature amplitude were matched to those described above (rise time = 5 ms; A_F = 9°; A_N = 0.48°). In an example cell recorded in the awake animal, there was a higher spontaneous firing rate than in the anesthetized animal, but spontaneous bursting prior to feature presentation was present (Figure 1F; not adapted). In the adapted condition, this neuron showed a reduction in number of feature-evoked spikes as well as a reduction in the feature-evoked bursting (Figure 1F; adapted). Consistent with the anesthetized findings, sensory adaptation in the awake rat led to a reduction in the overall number of feature-evoked spikes (data not shown). Comparing the bursting in the not adapted and adapted conditions in single-unit neurons recorded in the awake animal also revealed the same basic trend of a reduction in bursting with adaptation as

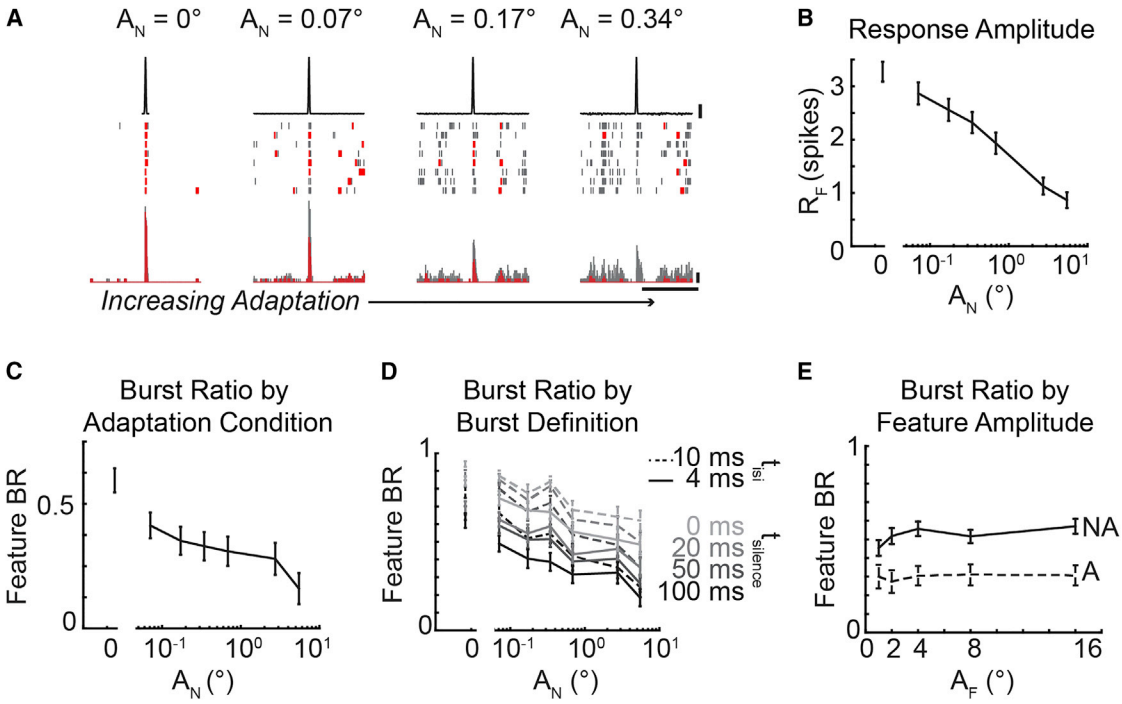

Figure 2. Thalamic Bursting Is Continuously Modulated by Sensory Adaptation

(A) Example neural response to increasing adapting noise amplitudes (A_F = 16°; A_N = 0°, 0.17°, 0.34°, and 0.7°). The scale bars represent 4°, 100 Hz, and 250 ms.

(B) Feature-evoked response across adaptation conditions (A_F = 16°; n = 44 cells; mean ± SEM).

(C) Feature burst ratio across adaptation conditions (A_F = 16°; n = 44 cells; mean ± SEM).

(D) Feature burst ratio across adaptation conditions defined using alternate burst definitions ($t_{silence}$: 0, 20, 50, and 100 ms; t_{isi}: 4 and 10 ms; n = 44 cells; mean ± SEM).

(E) Feature burst ratio in single adaptation condition across feature amplitudes (n = 26; mean ± SEM).

seen in the larger data set of the anesthetized animal (Figure 1G, green; n = 7 cells). However, the absolute level of bursting in the awake animal was reduced relative to the anesthetized animal. Importantly, the level of bursting seen in both the anesthetized and the awake animal was significantly greater than that expected by chance from a Poisson model neuron with an inhomogeneous firing rate that matches the evoked peristimulus time histogram measured experimentally (Figure 1G, green and black shaded regions with boundaries shown as tick marks on axes; see Supplemental Experimental Procedures).

Adaptation Modulates Burst/Tonic Firing on a Continuum

Whereas the dichotomy of burst/tonic firing in neural coding has often been described as a switch between thalamic states (Steriade et al., 1993), it has been shown that the thalamus actually operates in a graded fashion (Mukherjee and Kaplan, 1995). However, how this transition between the burst and tonic firing modes is influenced by external stimulation has not been explored. To investigate the role of the adapting noise stimulus on the feature-evoked bursting activity, we systematically varied the amplitude of the adapting noise (Figure 2A, example neuron). In the not adapted condition, the feature elicited burst firing from this neuron (Figure 2A; A_F = 16°; A_N = 0°). As the amplitude of the adapting noise stimulus increased, the amplitude of the feature-evoked response and the amount of burst firing decreased for this example neuron (Figure 2A; A_N = 0.07°, 0.17°, and 0.34°). Across cells, the response to the feature (R_F) decreased monotonically with increasing adapting noise stimulus amplitudes, consistent with increasing noise amplitudes leading to increasing degrees of adaptation (Figure 2B; A_F = 16°; n = 44 cells). However, the continuous decrease in the burst ratio with increasing adaptation intensity across cells (Figure 2C; n = 44 cells) quantified the reduced number of burst spikes to the overall reduction in the total number of evoked spikes. This continuum confirms that the thalamus can indeed operate in a graded fashion between burst and tonic firing, rather than in two discrete states of burst or tonic firing, and that this continuum can be modulated through sensory adaptation.

With increasing levels of adaptation, thalamic neurons were driven more strongly prior to feature presentation (example cell; Figure 2A). It is possible that the increase in firing rate due to ongoing stimulation during adaptation simply induced spiking activity in the 100-ms period of silence prior to the first spike of a burst ($t_{silence}$; Figure 1E) and therefore precluded classification as a burst in this context. To investigate whether the trend of reduced bursting with increasing adapting noise amplitude was simply due to increased noise-driven spiking, we systematically varied the definition of a burst to reduce the duration of

silence prior to the first spike ($t_{silence}$ = 0, 20, 50, and 100 ms) used to classify a series of spikes with short interspike intervals (t_{isi} = 4 ms) as a burst. Whereas reducing the duration of $t_{silence}$ led to a larger number of spikes being classified as burst spikes (and therefore quantitatively larger mean burst ratios across 44 cells), there were continuous reductions in the burst ratio regardless of the burst definition (Figure 2D, solid lines; n = 44 cells). We further altered our burst definition to allow the interspike interval for spikes within a burst to occur within 10 ms (t_{isi} = 10 ms; $t_{silence}$ = 0, 20, 50, and 100 ms) and again found that the burst ratio decreased with increasing noise amplitude (Figure 2D, dashed lines; n = 44 cells). This control analysis demonstrates that the modulation of burst ratio was not dependent on the specific burst definition. However, the underlying mechanisms of the channel suggest that a prolonged period of hyperpolarization is critical to the function of burst spikes because it primes T-type calcium channels to open and allows depressing synapses to recover from previous spiking activity (Sherman, 2001).

It is also possible that the amount of elicited bursting could actually be a function of the sensory feature used to probe the pathway rather than the state of the thalamus. By holding the statistics of the adapting noise stimulus constant and varying the feature, we found that the burst ratio was approximately constant across feature amplitudes. Importantly, this suggests that the bursting activity is a function of the ongoing sensory stimulation rather than the feature itself (Figure 2E; n = 26 cells).

Depolarization as an Adaptive Mechanism to Modulate Bursting

When a thalamic neuron is in a hyperpolarized state, an incoming depolarizing signal will activate the T-type calcium channels to allow an influx of calcium, which transiently depolarizes the neuron and permits burst firing (Perez-Reyes, 2003). By contrast, a net depolarization of the baseline membrane potential of the thalamic neuron inactivates the T-type calcium channel such that an incoming excitatory signal will not elicit the calcium-based wave of depolarization. Although the thalamic membrane potential is constantly fluctuating on a millisecond by millisecond timeframe as incoming signals transiently excite or inhibit a cell, it is the slower fluctuations of the cell membrane on the order of tens or hundreds of milliseconds that transitions the cell between different operating regimes. Thus, the reduction in feature-evoked burst firing with adaptation observed here suggests that the adapting stimulus may be inducing a sustained depolarization of the thalamic neurons and that this depolarization is sufficient to inactivate the T-type calcium channels.

To test this more directly, we transfected VPm neurons with a depolarizing opsin (ChR2(H134R)) and directly manipulated the baseline membrane potential using continuous blue light stimulation administered through an optic fiber lowered directly into VPm (λ = 470 nm; 0.5 mW/mm^2). We recorded sensory feature-evoked activity in three conditions: in the absence of any adapting stimulus or optogenetic manipulation (not adapted); in the presence of an adapting stimulus but absence of optogenetic manipulation (adapted); and in the presence of an optogenetic depolarization but absence of adapting stimulus (depolarized not adapted). Note that the ChR2 is being utilized as a modulating input, as compared to a driving input. As with the onset of the adapting noise stimulus, the onset of the optical stimulus would strongly drive neural activity initially, but the firing rate reached steady state within approximately 500 ms, after which we performed our measures (Figure S1A).

In an example cell, both artificial depolarization and sensory adaptation reduced the bursting in response to the feature (Figure 3A; depolarized not adapted, adapted; red, burst; gray, tonic) compared to the evoked response in the absence of the depolarizing optical input or the sensory adaption (Figure 3A; not adapted). Across cells, direct control of the baseline membrane potential of the thalamic neurons was sufficient to shift the feature-evoked thalamic firing along the burst/tonic continuum (Figure 3C; n = 12 cells) in a very similar manner to the burst/tonic transition for a range of adaptation levels (Figure 3B; n = 12 cells). Although the firing rate prior to feature presentation ($R_{N,L}$) remained low across the adaptation and light conditions (Figures 3D and 3E, dashed lines; n = 12 cells), we performed an additional control analysis to confirm the reduction of bursting activity with increasing light and adaptation conditions regardless of firing activity prior to feature presentation (Figure S1B).

Although the shift in bursting activity aligned well between the adaptation and light conditions, the evoked response to the feature did not. Consistent with the sensory adaption results in Figure 2B, increasing the amplitude of the adapting sensory noise stimulus led to a dramatic reduction in the feature-evoked neural response (Figure 3D). In contrast, increasing the depolarizing light input did not significantly reduce the feature-evoked thalamic responses (Figure 3E). This suggests that a net depolarization is sufficient to explain the decrease in bursting but that there may be a secondary mechanism by which the adapting sensory stimulus reduced the amplitude of the feature-evoked response. Specifically, the optogenetic depolarization of the thalamic neurons will not directly impact activity at the presynaptic terminals. Given the potential for depression of the trigeminothalamic synapse (Deschênes et al., 2003), we hypothesize that the reduction in the evoked neural response seen for adaptation, but not optogenetic modulation, could be due to reduced sensory drive/synaptic input.

To further probe these mechanistic issues, a biophysically inspired integrate-and-fire model was constructed (see Supplemental Experimental Procedures). The IFBS model was an integrate-and-fire (IF) model neuron with an incorporated bursting mechanism (B) to represent a T-type calcium channel current (Lesica et al., 2006) and a subthreshold and spike-dependent history component (S) to represent activity-dependent effects (Ladenbauer et al., 2012). The simulated spiking activity of the IFBS model without simulated sensory drive consisted primarily of burst spikes, whereas the inclusion of the simulated noise stimulus induced more depolarized conditions and tonic firing (Figure 3F). Increasing amplitudes of adapting sensory noise led to monotonically increasing levels of depolarization of the subthreshold membrane potential in the IFBS model (Figure 3G). Consistent with the experimental adaptation data (Figure 2C), the IFBS model showed a continuous decrease in feature-evoked burst ratio and the evoked feature response with increasing adapting noise amplitude (Figures 3H and 3I, black).

Please cite this article in press as: Whitmire et al., Information Coding through Adaptive Gating of Synchronized Thalamic Bursting, Cell Reports (2016), http://dx.doi.org/10.1016/j.celrep.2015.12.068

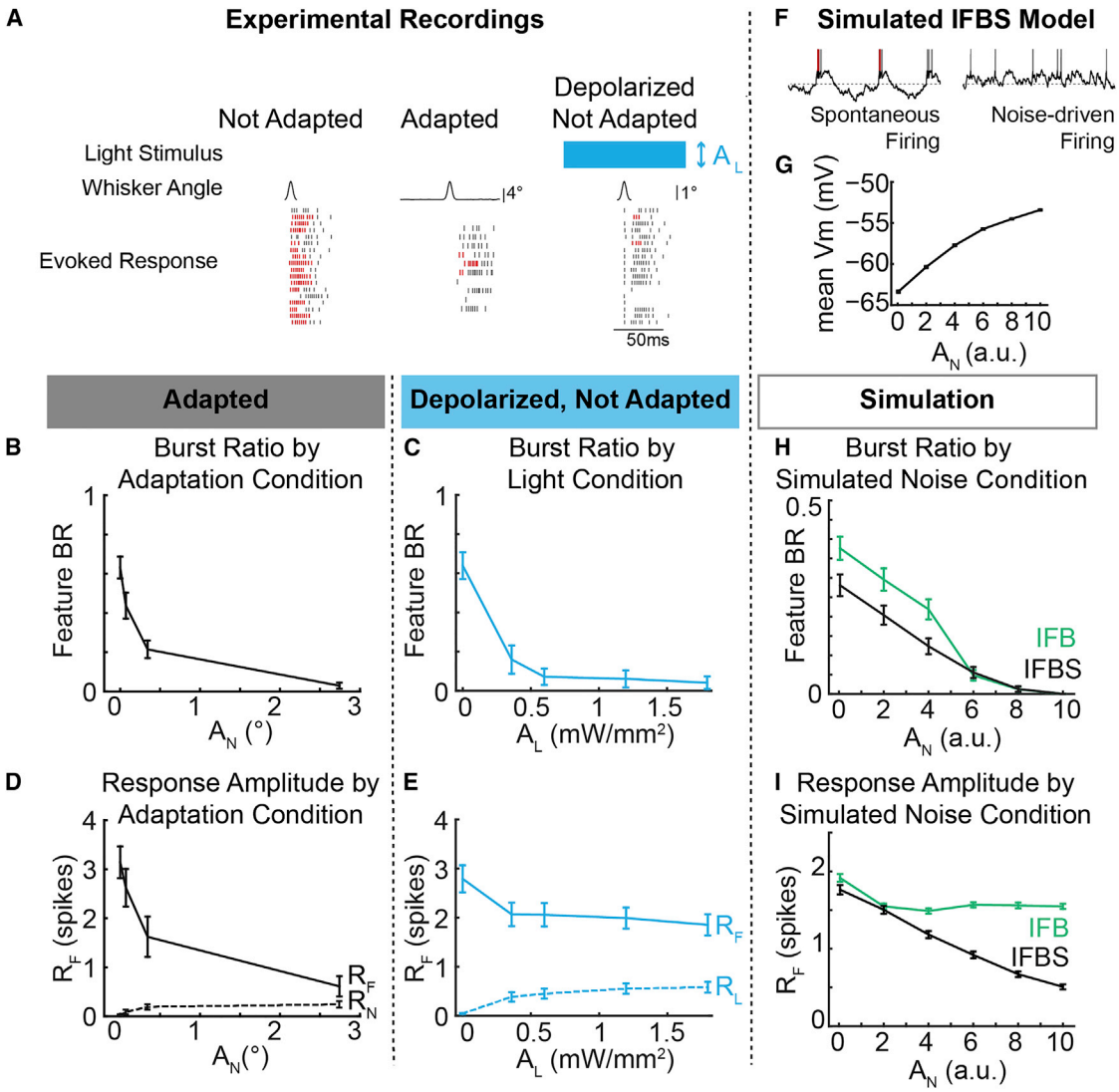

Figure 3. Direct Depolarization of Thalamic Neurons Shifts the Burst Ratio, but Not the Feature Encoding

(A) Example neuron response to the not adapted feature, the not adapted feature with modulating depolarization, and the adapted feature.

(B–E) Comparison of the feature burst ratio (B and C) and evoked feature response (D and E) to adapted sensory features (A_F = 8°) presented in sensory noise (black; n = 12) and not adapted sensory features (2°) presented while directly depolarizing thalamic neurons using ChR2 (blue; n = 12). Responses to the noise (R_N) and light stimulation (R_L) prior to feature presentation are shown as dotted lines in (D) and (E). Error bars are SE.

(F) Example simulated membrane potentials from an IFBS model with and without simulated sensory input.

(G) Mean simulated membrane potential across simulated noise amplitudes in an IFBS model (n = 250 trials).

(H and I) Comparison of the burst ratio (H) and feature response (I) to simulated sensory features presented in sensory noise with an IFBS model (black; n = 250 trials) and an IFB model (green; n = 250 trials). Error bars are SE.

However, the development of the IFB model through the removal of the subthreshold and spike-dependent history component (S) more closely mimicked the experimental optogenetics results. Similar to the IFBS model, the IFB model experienced increasing levels of depolarization with increasing noise amplitudes (data not shown) and was able to recreate a continuous modulation of bursting activity with increasing simulated noise amplitudes (Figure 3H, green). In contrast to the adaptation data and in agreement with the optogenetic data, the IFB model actually maintained the evoked feature response due to the lack of any spiking history dependence (Figure 3I, green).

Taken together, these experimental and simulated results suggest that sensory noise adaptation may be affecting bursting activity by depolarizing the thalamic neurons and inactivating the T-type calcium channels. However, the inability of depolarization through optogenetic modulation and the IFB model to mimic the reduction in the evoked feature response seen with increasing noise amplitudes suggests that depolarization of the cell membrane alone is insufficient to fully explain the mechanism

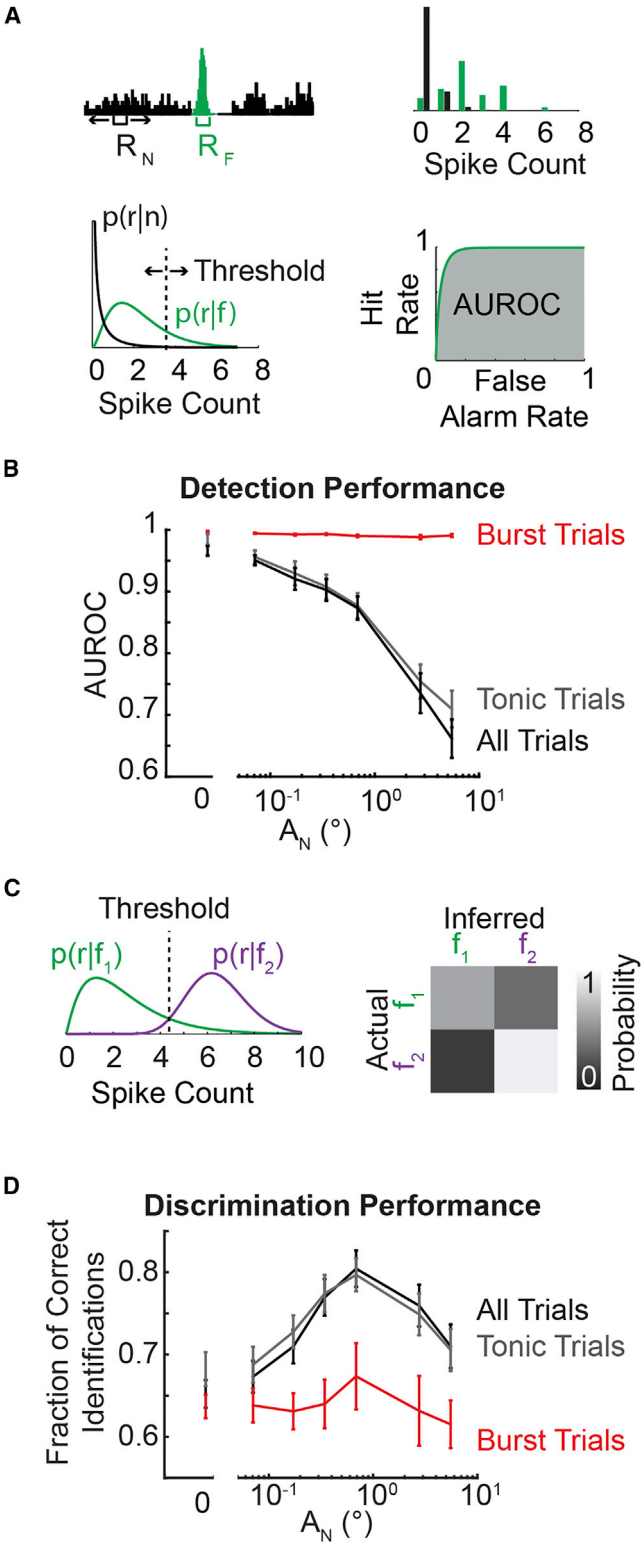

Figure 4. Adaptation Shifts Encoding from Detection to Discrimination Mode

(A) Schematic depicting the quantification of the evoked response to the noise (R_N) and the feature (R_F) and the estimation of a probability distribution that can be parameterized. Detectability was quantified as the area under the receiver operator characteristic's curve (AUROC).

(B) Detectability (AUROC) across adaptation conditions for all trials, burst trials, and tonic trials (black, red, and gray lines, respectively; n = 44 cells; A_F = 16°; mean ± SEM).

(C) Schematic depicting the probability distributions for two different features (A_F = 2° and 16°) and the threshold set using a maximum likelihood estimator. The performance matrix estimated the fraction of correct identifications.

(D) The discriminability (fraction of correct identifications) across adaptation conditions for all trials, burst trials, and tonic trials (black, red, and gray lines, respectively; n = 44 cells; A_F = 16°; mean ± SEM).

underlying sensory adaptation. Given the qualitative alignment of the burst ratio and feature-evoked response of the IFBS simulations and the experimental sensory adaptation data, we suggest that one combination of mechanisms by which sensory adaptation could be acting is through thalamic membrane depolarization to modulate bursting paired with reduced efficacy of the sensory drive due to activity-dependent synaptic effects to modulate evoked feature responses.

Functional Consequences of Shifts in Burst/Tonic Firing

Thalamic firing modes have profound implications for the transmission of information from the thalamus to cortex. Burst spikes have shown enhanced but highly nonlinear probability of eliciting a spike in a monosynaptically connected downstream cortical neuron (Swadlow and Gusev, 2001), whereas tonic spikes are believed to maintain a more-linear relationship between stimulus intensity and elicited response (Sherman, 2001). As such, adaptive gating of thalamic firing modes represents a potentially profound mechanism of modulating information transmission.

Using an ideal observer of thalamic spiking activity, we quantified the effect of increasing adapting noise levels on the detectability of a single feature or the discriminability between two features from the thalamic spiking. Thalamic responses were quantified as the number of spikes elicited in response to the feature (R_F) and to the adapting noise (R_N) in a 10-ms window (Figure 4A, top left). Spike count probability distributions were estimated from the observed thalamic spike counts (Figure 4A, top right). Using parameterized distributions (Figure 4A, bottom left; see Supplemental Experimental Procedures), a sliding threshold was used to compute a receiver operator characteristics (ROC) curve (Figure 4A, bottom right). The ROC curve represents the probability of a false alarm versus the probability of a correct detection (hit). The area under the ROC curve (AUROC) was used as a metric of detectability where an AUROC value of 1 corresponds to a perfect detector and an AUROC value of 0.5 corresponds to complete overlap of the feature and noise distributions (p(r|f) and p(r|n), respectively). With increasing adaptation, the detectability of the feature monotonically decreased for all trials (Figure 4B, black). However, when the trials were parsed such that "burst trials" corresponded to trials where the response to the feature resulted in burst firing and "tonic trials" corresponded to trials where the response to the feature resulted in tonic firing, it was evident that burst trials remained highly detectable regardless of the adaptation condition (Figure 4B, red). However, the high detectability of burst trials had a limited effect on the overall detectability (Figure 4B, black)

Please cite this article in press as: Whitmire et al., Information Coding through Adaptive Gating of Synchronized Thalamic Bursting, Cell Reports (2016), http://dx.doi.org/10.1016/j.celrep.2015.12.068

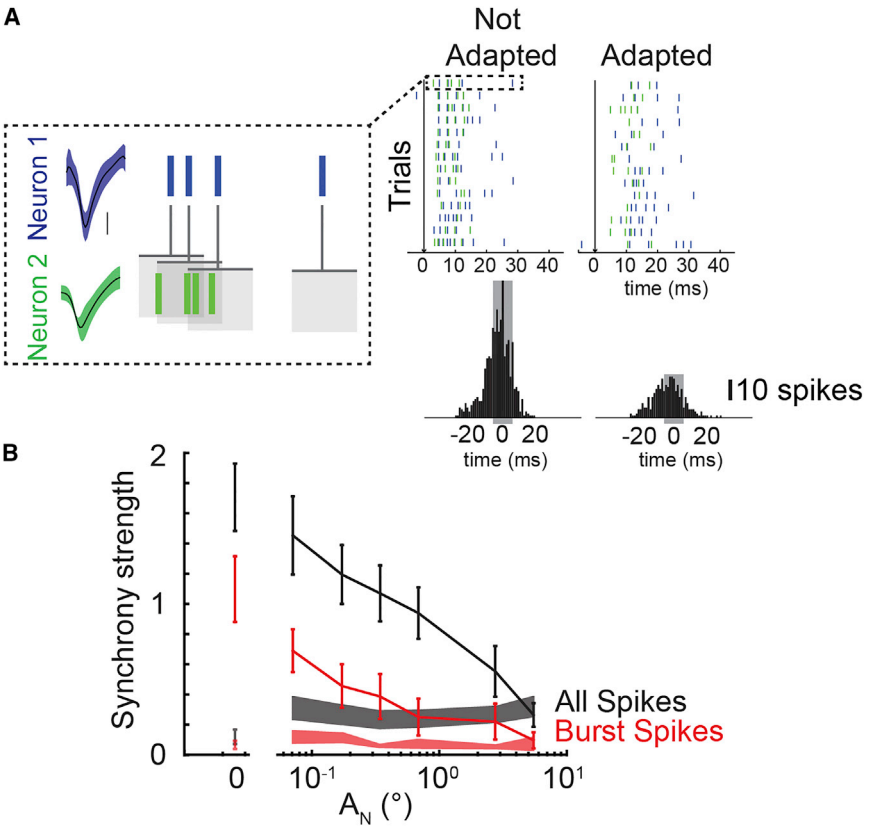

Figure 5. Adapting Sensory Noise Modulates Synchrony of Thalamic Bursting

(A) Example neuron pair response to feature (t = 0 ms; black arrow) presented in an adapted and not adapted condition (A_N = [0, 0.3433]°; A_F = 16°). The scale bar represents 100 μV. One example trial is shown in the dotted box whereby the spike times from neuron 2 were rearranged relative to neuron 1 to build the cross-correlogram shown beneath the two noise stimulus conditions. Synchrony strength was defined as the number of spikes within a ± 5 ms window of the cross-correlogram (gray shading) normalized by the number of spikes from each neuron.

(B) Synchrony of all feature-evoked spikes (black) and feature-evoked burst spikes (red) across adapting stimulus amplitude (n = 12 pairs; mean ± SEM). The synchrony of noise-evoked spikes across cells is shown as shaded bars (black, all noise-evoked spikes; red, all burst-evoked spikes; mean ± SEM). Spontaneous synchrony is shown as a shaded bar at A_N = 0.

due to the reduction in the absolute number of burst trials with increasing noise amplitudes (Figure 2C).

Furthermore, the ability of an ideal observer to discriminate between two different stimulus features (A_F = 2° and 16°) was quantified. As described above, the response distribution for each feature amplitude was estimated from the spiking activity of the thalamic neuron (Figure 4C, left). A response threshold was identified using a maximum likelihood framework such that an observer would infer which stimulus was presented by selecting the stimulus for which the likelihood $p(r|f_i)$ is maximized. Discrimination performance was quantified using a performance matrix whereby the accuracy of the observer is compared to the correct stimulus classification (Figure 4C, right). Given that the ideal observer was discriminating between two feature amplitudes, operating at chance corresponds to a correct identification probability of 0.5. The discriminability was maximized across all trials at an intermediate level of adaptation (Figure 4D, black). However, the discrimination performance for only burst trials (Figure 4D, red) remained lower than the discrimination performance across all trials or only tonic trials (Figure 4D, black and gray, respectively), consistent with the view that bursting is better for strong activation than for descriptive signaling (Sherman, 2001).

Thalamic Synchrony and Bursting

Cortical neurons are particularly sensitive to the timing of spiking inputs within and across cells due to weak thalamocortical synapses paired with the narrow cortical integration window, mediated by the disynaptic feedforward inhibition (Gabernet et al., 2005). Synchronous firing across thalamic neurons has been identified as a mechanism to overcome the weak synaptic strength of thalamocortical connections to send strong suprathreshold inputs to cortex (Bruno and Sakmann, 2006). To assess the effects of increasing degrees of adaptation on population synchronization and bursting, we used a multi-electrode drive to simultaneously record from pairs of thalamic neurons with two electrodes residing within the same barreloid. Electrodes were independently controlled, and latencies in response to single whisker stimuli were tested to ensure proper localization (A_F = 16°; FSL = 6.6 ± 0.6 ms; R_F = 3.37 ± 0.2 spikes; n = 12 pairs of neurons; all data from synchronously recorded neurons [n = 24] are also included in single-unit responses presented in Figures 2 and 4). In an example pair of neurons, a feature presented without adaptation elicits a large number of spikes with a short latency, as was observed for individual neuron recordings (Figure 5A; not adapted condition). To assess synchronous firing between these two neurons, we used correlation analysis to quantify the spiking activity of neuron 2 relative to neuron 1 (Figure 5A, dotted box). The cross-correlogram in the not adapted condition revealed a higher level of synchrony, or more-synchronous spikes within a ±5 ms window, than the cross-correlogram in the adapted condition (Figure 5A, gray-shaded region of cross-correlogram). Increasing levels of adaptation also led to a reduction in the number of spikes that were elicited in response to a sensory feature. To account for the reduction in overall spike count, the synchrony strength, quantified as the number of near-synchronous spikes within a ±5 ms window, was normalized by the number of spikes from each of the neurons (see Supplemental Experimental Procedures), thus providing a normalized measure of the number of near-synchronous spikes evoked by the stimulus.

Increasing levels of adapting noise amplitude (and thus degrees of adaptation) led to a continuous decrease in the synchrony strength between pairs of simultaneously recorded thalamic neurons (Figure 5B, black; n = 12 pairs). When only the synchrony of burst firing was considered, there was a similar reduction in feature-evoked burst spike synchrony with increasing noise amplitudes (Figure 5B, red line; n = 12 pairs), suggesting that adaptation modulates both burst firing within a single neuron and synchronous burst firing across pairs of neurons. Furthermore, the spontaneous synchrony for both total spiking activity and burst spiking alone in the absence of sensory stimulation was low relative to feature-evoked synchrony (Figure 5B, shaded lines at $A_{N} = 0$). The lack of spontaneous synchronous firing and synchronous burst firing further underscores the importance of sensory drive in synchronizing bursting activity in the thalamus. The synchrony in response to the noise stimulus was also relatively low and invariant to the amplitude of the noise (Figure 5B, shaded lines), demonstrating that thalamic neurons are not always synchronized.

DISCUSSION

Although thalamic bursting was originally identified in sleeping animals as a proposed mechanism to decouple thalamocortical activity from the peripheral world (Steriade et al., 1993), recent evidence suggests that thalamic bursting plays a fundamental role in sensory processing and is evoked by naturally induced firing patterns (Wang et al., 2007). Significant work in the visual pathway has explored the role of thalamic bursting in information transmission, where it has been hypothesized that thalamic state, as quantified by the intrinsic membrane potential of the thalamic neurons, is responsible for switching the encoding, or "gating," mechanism of the thalamus from a burst to a tonic firing mode (Sherman, 1996). However, in natural sensing conditions, organisms are faced with a continuous stream of sensory stimuli with relevant information embedded intermittently rather than a simple presence or absence of relevant sensory information. Here, we have shown that the state of the thalamus is continuously modulated by ongoing sensory activity, allowing graded transitions between synchronous bursting and asynchronous tonic firing regimes. Although present at lower rates than observed in the anesthetized state, previous studies from both the visual (Bezdudnaya et al., 2006; Guido and Weyand, 1995) and somatosensory (Swadlow and Gusev, 2001) pathways have demonstrated the presence of thalamic bursting in awake, attentive states, suggesting a potential role for burst modulation in sensory perception. However, further studies are needed to further elucidate this in the context of behavior.

Although the precise role of sensory adaptation is still debated, it is largely accepted that adaptation serves a beneficial purpose as opposed to just fatigue (Wark et al., 2007). Adaptive gain control has been proposed as one mechanism to promote efficient coding by adjusting the operating range for inputs based on recent stimulus history (Fairhall et al., 2001; Maravall et al., 2007). Our results suggest that sensory adaptation goes beyond a change in operating points for the neurons by providing a relevant mechanism for fundamentally shifting sensory-evoked bursting activity along a continuum of values based entirely on the subthreshold activity of the thalamic neurons, resulting in dramatic changes in feature selectivity. Simple gain scaling will be further amplified by the nonlinear response properties of thalamic neurons as they transition between varying states of the burst/tonic continuum.

The ideal observer analysis of thalamic spiking activity demonstrates the functional effect of adaptation on detectability loss but discriminability gain, consistent with prior electrophysiological and behavioral studies (Ollerenshaw et al., 2014; Wang et al., 2010; Zheng et al., 2015). When parsing the trials by the presence or absence of a feature-evoked burst, the detectability of burst responses remained high regardless of adaptation condition, as suggested by the view of burst spikes as sending a strong signal to cortex (Guido et al., 1995). However, the transmission of a thalamic spike downstream is entirely dependent on the thalamocortical synapse. The long period of hyperpolarization, required to de-inactivate the T-type calcium channels and prepare them to open, plays an additional role in information transmission by permitting the depressing thalamocortical synapse to recover from previous spiking activity (Swadlow and Gusev, 2001). Furthermore, the high-frequency burst of spiking becomes a strong driving input to a cortical neuron that will integrate thalamic spiking activity within a short window, known as the cortical window of integration (Wang et al., 2010). Whereas the size of this window is dependent on prior thalamic activity and is relatively short for not adapted probes, the cortical integration window in barrel cortex extends to approximately 10 ms in duration after repetitive stimulation (Gabernet et al., 2005). The importance of not only burst firing within a single neuron, but synchronous burst firing across neurons, is further underscored by the fact that cortical neurons are integrating spiking information from many thalamic neurons simultaneously within this cortical window of integration (Bruno and Sakmann, 2006).

Importantly, we have shown that synchronous firing across neurons is stimulus driven. In the absence of sensory stimulation, high levels of synchronous firing have been associated with the anesthetized or sleeping state (Steriade et al., 1993). However, our results show that neither burst nor tonic spiking was spontaneously synchronous across neurons in the fentanyl-anesthetized rat, consistent with findings from the awake rabbit (Swadlow and Gusev, 2001). Instead, we found that synchronous bursting was only elicited by strong sensory stimulation, suggesting that this pattern of activity is reserved for sensory-driven responses.

Whereas it is likely that several biophysical mechanisms underlie the adaptation effects seen extracellularly, we specifically investigated net depolarization effects as a mechanism to modulate bursting activity. Although the thalamus receives strong driver inputs from the peripheral whisker sensors via the brainstem, the majority of the synapses on thalamic neurons originate in cortex (Varela, 2014). In addition, recent evidence has shown that direct corticothalamic feedback onto VPm neurons can lead to a sustained depolarization of the baseline membrane potential (Crandall et al., 2015; McCormick and von Krosigk, 1992; Mease et al., 2014). As such, depolarization via corticothalamic feedback is a strong candidate mechanism for cortical control of thalamic state. However,

Please cite this article in press as: Whitmire et al., Information Coding through Adaptive Gating of Synchronized Thalamic Bursting, Cell Reports (2016), http://dx.doi.org/10.1016/j.celrep.2015.12.068

the net depolarization induced by optogenetic currents alone was insufficient to explain the reduction in the evoked sensory feature response. We hypothesize that adaptation is acting through multiple mechanisms, including subthalamic changes, to modulate the thalamic encoding. The reduced sensory drive/synaptic input could be due to adaptation effects in subthalamic processing such as depression of the trigeminothalamic synapse (Deschênes et al., 2003). Whereas our modeling results suggest that a net depolarization and reduced neural drive presents one possible explanation for our findings, there are likely multiple other mechanisms by which adaptation is modulating thalamic encoding. In particular, the adapting stimulus presented a noisy context surrounding the embedded feature that likely evokes significant changes in synaptic background activity. Evidence from in vitro recordings suggests that the synaptic noise, also potentially mediated by corticothalamic feedback, will significantly change the level of bursting in thalamic neurons (Wolfart et al., 2005). In the awake behaving animal, there will also be significant alterations to thalamic encoding due to neuromodulatory inputs as well as behavioral state fluctuations (Castro-Alamancos and Gulati, 2014; Niell and Stryker, 2010), which further highlights the abundance of neural mechanisms to alter thalamic state.

In the visual pathway, sensory-evoked bursting activity in the thalamus has been proposed to be well suited for detecting change in the visual scene (Lesica and Stanley, 2004; Lesica et al., 2006; Wang et al., 2007). Paired with results from the somatosensory pathway presented here, the effect of burst/tonic firing on information encoding appears consistent between the sensory modalities such that bursts are highly detectable whereas tonic firing maintains a more linear input-output function. Furthermore, sensory encoding in both the visual and somatosensory pathways is extremely precise (Butts et al., 2007; Petersen et al., 2008), suggesting an important role for temporal coding in both pathways. However, the temporal dynamics of feature selectivity of thalamic neurons in the somatosensory pathway are significantly faster than those in the visual pathway (full width of half maximum of the temporal receptive field of approximately 3.5 ms versus 20 ms, respectively; Lesica et al., 2007; Petersen et al., 2008) and somatosensory detection tasks support near-instantaneous encoding rather than sensory integration (Waiblinger et al., 2015a, 2015b), suggesting that bursting in the somatosensory pathway may be critical for rapid touch encoding. There are also some differences in the anatomical connectivity of these two sensory pathways. Within thalamus, both visual and somatosensory thalamic relay nuclei receive inhibitory input from the reticular nucleus, but the visual thalamus also incorporates inhibitory input from interneurons. The reticular thalamus provides a strong level of inhibitory tone (Halassa et al., 2014; Pinault, 2004) whereas interneurons within visual thalamus are hypothesized to play a role in shaping feature selectivity in the pathway (Butts et al., 2011). The absence or presence of inhibitory interneurons could play an important role in determining both the temporal dynamics of the feature selectivity and the burst response properties of the excitatory thalamocortical neurons in these sensory pathways (Alitto et al., 2005; Denning and Reinagel, 2005; Lesica and Stanley, 2004).

Beyond the primary sensory pathway, the processing of somatosensory information is also influenced by motor signals during active touch (Hentschke et al., 2006). Whereas all stimuli in this study were presented passively, previous studies with passive whisker stimulation embedded in active whisking conditions have shown a dependency of the evoked cortical response on the whisking state of the animal (Crochet and Petersen, 2006; Fanselow and Nicolelis, 1999). Furthermore, exploratory whisker behavior can involve complex spatiotemporal patterns at the whisker pad due to multiple whiskers repeatedly contacting an object (Sachdev et al., 2001). The passive single-whisker stimulation paradigm used here, which did not incorporate motor control or complex spatiotemporal whisker patterns, provided a simplified paradigm to systematically characterize the relationship between sensory adaptation and thalamic state. However, we would hypothesize that additional sensorimotor cortical and sub-cortical circuits, as well as the complex dynamics of the sensory stimulation, play a fundamental role in shaping the processing of somatosensory information at multiple levels of the pathway. Whereas the potential role of motor feedback on processing in the somatosensory cortex has been identified (Ferezou et al., 2007; Zagha et al., 2013), the implications for sub-cortical processing remain unknown.

Ultimately, our results link ongoing sensory stimulation with continuous modulations in thalamic state, as evidenced by the synchronous bursting activity. Adaptive alterations to the firing patterns in thalamus have profound implications for thalamic feature selectivity (Lesica et al., 2006), thalamocortical efficacy (Swadlow and Gusev, 2001), and functional encoding properties (Wang et al., 2010). The ability of sensory adaptation to shift thalamic firing patterns along a continuum of patterns opens up a dynamic interplay between the incoming sensory information and the demands on the system that allows for flexible encoding. Although the adaptive state modulation shown here could be mediated by corticothalamic feedback from primary somatosensory cortex, providing a sustained depolarizing drive to thalamic neurons, additional work is required to understand how different mechanisms, such as adaptation, active sensing, and neuromodulatory inputs, interact in the context of state-dependent encoding. Taken together, the deeply interconnected thalamocortical loop could be performing significant processing in a non-feedforward manner with modulating inputs from multiple brain regions.

EXPERIMENTAL PROCEDURES

Acute Surgery

All procedures were approved by the Georgia Institute of Technology Institutional Animal Care and Use Committee and were in agreement with guidelines established by the NIH. Nineteen female albino rats (Sprague-Dawley; 250–300 g) were used for these experiments (n = 14 naive animals; n = 5 optogenetically modified animals). The fentanyl-cocktail anesthesia (fentanyl [5 μg/kg], midazolam [2 mg/kg], and dexmedetomidine [150 μg/kg]) was continuously administered intravenously using a drug pump throughout the duration of the experiment.

Electrophysiology

Tungsten microelectrodes (70 μm diameter; 2 MΩ impedance; FHC) or quartz-insulated platinum/tungsten microelectrodes (95%/5%; 2 MΩ impedance; Thomas Recording) were lowered into the brain (depth: 4.5–6 mm) using a

hydraulic micropositioner (Kopf) to record extracellularly from VPm neurons. Multiple single-unit recordings were performed using independently controllable electrodes (Mini Matrix Drive; Thomas Recordings). Recordings were made using a 32-channel Plexon data acquisition system (Plexon) or a 64-channel TDT data acquisition system (Tucker Davis Technologies). The topographic location of the electrode was identified through manual stimulation of the whisker pad. Upon identification of a whisker-sensitive single unit, the primary whisker was threaded into the galvo motor to permit stimulation of a single whisker.

Sensory Stimulus

Mechanical whisker stimulation was delivered using a precisely controlled galvo motor (Cambridge Technologies). The galvo motor was controlled using custom software (Matlab; Mathworks) to provide millisecond precision. The mechanical stimulus applied to the whisker in the rostral-caudal direction consisted of features (5 ms rise time; amplitude of the feature [A_F] = 0.25°, 0.5°, 1°, 2°, 4°, 8°, and 16°) embedded in two conditions: without background noise and with white noise background (low pass filtered at 200 Hz due to mechanical limitations of the galvo motor; SD of the noise [A_N] = 0°, 0.025°, 0.07°, 0.172°, 0.343°, 0.6854°, 2.7432°, and 5.485°). The feature was designed as a Gaussian waveform (10 ms duration). To generate different velocity stimuli, the amplitude of the feature was changed while the temporal duration remained fixed. The noise was silenced at the feature locations. Each noise epoch had a catch trial with silenced noise but no feature (negative control). Different noise amplitudes were interleaved to avoid long-term adaptation effects.

Optogenetic Stimulus

Optical manipulation was administered with a controlled pulse of light from a blue LED through a custom optrode consisting of an optical fiber (200 μm diameter; Thorlabs) and an electrode (tungsten microelectrode; FHC) that was lowered into the VPm. Upon identifying a whisker-sensitive cell, light sensitivity was assessed using a train of 10-Hz light pulses (λ = 470 nm). The optical and whisker stimulus consisted of a feature (A_F = 1° and 8°) embedded in 750-ms square light pulses (0, 0.36, 0.6, 1.2, and 1.8 mW/mm^2).

Awake Electrophysiology

All experimental and surgical procedures were carried out in accordance with standards of the Society of Neuroscience and the German Law for the Protection of Animals. Awake electrophysiological recordings were obtained from two female albino rats (Sprague-Dawley). The basic procedures for headcap surgery, habituation to head fixation, and behavioral training followed previously published methods (Schwarz et al., 2010). Electrophysiological recordings were obtained while the rats were performing a detection of change task (Waiblinger et al., 2015a).

Analytical Methods

Spike sorting was performed online using negative threshold crossing at least two SDs above the noise and online sorting of the recorded waveforms. The sorting results performed online were validated offline using Waveclus (Quiroga et al., 2004). Isolation of the unit was confirmed by the waveform amplitude (absolute and relative to the background noise) and the interspike-interval distributions. FSL was defined as the first spike fired during the neural response window on each trial. FSL jitter was defined as the SD of the FSL across trials. The amplitude of the response to the sensory feature was defined as the number of elicited spikes in a sliding 10-ms window following feature presentation. Synchronous firing was quantified by the synchrony strength (Temereanca et al., 2008). Ideal observer analysis of thalamic spiking activity was performed on the probability distributions of the number of spikes elicited in response to sensory features (p(r|f)) and sensory noise (p(r|n)) estimated from the observed spike counts (Wang et al., 2010). Additional details can be found in the Supplemental Experimental Procedures.

Computational Model

An integrate-and-fire model with a bursting mechanism (IFB model) was developed using previously published models in vision (Lesica et al., 2006). An additional spike history component was added to simulate the effect of ongoing stimulation (IFBS model; Ladenbauer et al., 2012). Simulated neural responses were analyzed using the same techniques described for experimental data. The full model can be found in the Supplemental Experimental Procedures.

SUPPLEMENTAL INFORMATION

Supplemental Information includes Supplemental Experimental Procedures and one figure and can be found with this article online at http://dx.doi.org/10.1016/j.celrep.2015.12.068.

AUTHOR CONTRIBUTIONS

Conceptualization, C.J.W., C.W., C.S., and G.B.S.; Methodology, C.J.W.; Investigation, C.J.W. and C.W.; Writing – Original Draft, C.J.W. and G.B.S.; Writing – Reviewing & Editing, C.J.W., C.W., C.S., and G.B.S.

ACKNOWLEDGMENTS

This work was supported by US-German Collaborative Research in Computational Neuroscience grant (US: NSF CRCNS IOS-1131948; German: BMBF CRCNS 01GQ1113) and NIH National Institute of Neurological Disorders and Stroke grants R01NS048285 and R01NS085447. C.J.W. was supported by GT/Emory NIH Computational Neuroscience Training grant T90DA032466 and the NIH NRSA pre-doctoral fellowship F31NS089412.

Received: July 13, 2015
Revised: October 7, 2015
Accepted: December 11, 2015
Published: January 14, 2016

REFERENCES

Ahissar, E., Sosnik, R., and Haidarliu, S. (2000). Transformation from temporal to rate coding in a somatosensory thalamocortical pathway. Nature *406*, 302–306.

Alitto, H.J., Weyand, T.G., and Usrey, W.M. (2005). Distinct properties of stimulus-evoked bursts in the lateral geniculate nucleus. J. Neurosci. *25*, 514–523.

Bezdudnaya, T., Cano, M., Bereshpolova, Y., Stoelzel, C.R., Alonso, J.-M., and Swadlow, H.A. (2006). Thalamic burst mode and inattention in the awake LGNd. Neuron *49*, 421–432.

Bruno, R.M., and Sakmann, B. (2006). Cortex is driven by weak but synchronously active thalamocortical synapses. Science *312*, 1622–1627.

Butts, D.A., Weng, C., Jin, J., Yeh, C.I., Lesica, N.A., Alonso, J.M., and Stanley, G.B. (2007). Temporal precision in the neural code and the timescales of natural vision. Nature *449*, 92–95.

Butts, D.A., Weng, C., Jin, J., Alonso, J.M., and Paninski, L. (2011). Temporal precision in the visual pathway through the interplay of excitation and stimulus-driven suppression. J. Neurosci. *31*, 11313–11327.

Castro-Alamancos, M.A., and Gulati, T. (2014). Neuromodulators produce distinct activated states in neocortex. J. Neurosci. *34*, 12353–12367.

Crandall, S.R., Cruikshank, S.J., and Connors, B.W. (2015). A corticothalamic switch: controlling the thalamus with dynamic synapses. Neuron *86*, 768–782.

Crick, F. (1984). Function of the thalamic reticular complex: the searchlight hypothesis. Proc. Natl. Acad. Sci. USA *81*, 4586–4590.

Crochet, S., and Petersen, C.C.H. (2006). Correlating whisker behavior with membrane potential in barrel cortex of awake mice. Nat. Neurosci. *9*, 608–610.

Dean, I., Harper, N.S., and McAlpine, D. (2005). Neural population coding of sound level adapts to stimulus statistics. Nat. Neurosci. *8*, 1684–1689.

Denning, K.S., and Reinagel, P. (2005). Visual control of burst priming in the anesthetized lateral geniculate nucleus. J. Neurosci. *25*, 3531–3538.

Deschênes, M., Timofeeva, E., and Lavallée, P. (2003). The relay of high-frequency sensory signals in the Whisker-to-barreloid pathway. J. Neurosci. *23*, 6778–6787.

Please cite this article in press as: Whitmire et al., Information Coding through Adaptive Gating of Synchronized Thalamic Bursting, Cell Reports (2016), http://dx.doi.org/10.1016/j.celrep.2015.12.068

Fairhall, A.L., Lewen, G.D., Bialek, W., and de Ruyter Van Steveninck, R.R. (2001). Efficiency and ambiguity in an adaptive neural code. Nature *412*, 787–792.

Fanselow, E.E., and Nicolelis, M.A. (1999). Behavioral modulation of tactile responses in the rat somatosensory system. J. Neurosci. *19*, 7603–7616.

Ferezou, I., Haiss, F., Gentet, L.J., Aronoff, R., Weber, B., and Petersen, C.C.H. (2007). Spatiotemporal dynamics of cortical sensorimotor integration in behaving mice. Neuron *56*, 907–923.

Gabernet, L., Jadhav, S.P., Feldman, D.E., Carandini, M., and Scanziani, M. (2005). Somatosensory integration controlled by dynamic thalamocortical feed-forward inhibition. Neuron *48*, 315–327.

Guido, W., and Weyand, T. (1995). Burst responses in thalamic relay cells of the awake behaving cat. J. Neurophysiol. *74*, 1782–1786.

Guido, W., Lu, S.M., Vaughan, J.W., Godwin, D.W., and Sherman, S.M. (1995). Receiver operating characteristic (ROC) analysis of neurons in the cat's lateral geniculate nucleus during tonic and burst response mode. Vis. Neurosci. *12*, 723–741.

Halassa, M.M., Chen, Z., Wimmer, R.D., Brunetti, P.M., Zhao, S., Zikopoulos, B., Wang, F., Brown, E.N., and Wilson, M.A. (2014). State-dependent architecture of thalamic reticular subnetworks. Cell *158*, 808–821.

Hentschke, H., Haiss, F., and Schwarz, C. (2006). Central signals rapidly switch tactile processing in rat barrel cortex during whisker movements. Cereb. Cortex *16*, 1142–1156.

Ladenbauer, J., Augustin, M., Shiau, L., and Obermayer, K. (2012). Impact of adaptation currents on synchronization of coupled exponential integrate-and-fire neurons. PLoS Comput. Biol. *8*, e1002478.

Lesica, N.A., and Stanley, G.B. (2004). Encoding of natural scene movies by tonic and burst spikes in the lateral geniculate nucleus. J. Neurosci. *24*, 10731–10740.

Lesica, N.A., Weng, C., Jin, J., Yeh, C.I., Alonso, J.M., and Stanley, G.B. (2006). Dynamic encoding of natural luminance sequences by LGN bursts. PLoS Biol. *4*, e209.

Lesica, N.A., Jin, J., Weng, C., Yeh, C.I., Butts, D.A., Stanley, G.B., and Alonso, J.M. (2007). Adaptation to stimulus contrast and correlations during natural visual stimulation. Neuron *55*, 479–491.

Lottem, E., and Azouz, R. (2008). Dynamic translation of surface coarseness into whisker vibrations. J. Neurophysiol. *100*, 2852–2865.

Lu, S.M., Guido, W., and Sherman, S.M. (1992). Effects of membrane voltage on receptive field properties of lateral geniculate neurons in the cat: contributions of the low-threshold Ca2+ conductance. J. Neurophysiol. *68*, 2185–2198.

Maravall, M., Petersen, R.S., Fairhall, A.L., Arabzadeh, E., and Diamond, M.E. (2007). Shifts in coding properties and maintenance of information transmission during adaptation in barrel cortex. PLoS Biol. *5*, e19.

McCormick, D.A., and von Krosigk, M. (1992). Corticothalamic activation modulates thalamic firing through glutamate "metabotropic" receptors. Proc. Natl. Acad. Sci. USA *89*, 2774–2778.

Mease, R.A., Krieger, P., and Groh, A. (2014). Cortical control of adaptation and sensory relay mode in the thalamus. Proc. Natl. Acad. Sci. USA *111*, 6798–6803.

Mukherjee, P., and Kaplan, E. (1995). Dynamics of neurons in the cat lateral geniculate nucleus: in vivo electrophysiology and computational modeling. J. Neurophysiol. *74*, 1222–1243.

Niell, C.M., and Stryker, M.P. (2010). Modulation of visual responses by behavioral state in mouse visual cortex. Neuron *65*, 472–479.

Ollerenshaw, D.R., Zheng, H.J.V., Millard, D.C., Wang, Q., and Stanley, G.B. (2014). The adaptive trade-off between detection and discrimination in cortical representations and behavior. Neuron *81*, 1152–1164.

Perez-Reyes, E. (2003). Molecular physiology of low-voltage-activated t-type calcium channels. Physiol. Rev. *83*, 117–161.

Petersen, R.S., Brambilla, M., Bale, M.R., Alenda, A., Panzeri, S., Montemurro, M.A., and Maravall, M. (2008). Diverse and temporally precise kinetic feature selectivity in the VPm thalamic nucleus. Neuron *60*, 890–903.

Pinault, D. (2004). The thalamic reticular nucleus: structure, function and concept. Brain Res. Brain Res. Rev. *46*, 1–31.

Quiroga, R.Q., Nadasdy, Z., and Ben-Shaul, Y. (2004). Unsupervised spike detection and sorting with wavelets and superparamagnetic clustering. Neural Comput. *16*, 1661–1687.

Reinagel, P., Godwin, D., Sherman, S.M., and Koch, C. (1999). Encoding of visual information by LGN bursts. J. Neurophysiol. *81*, 2558–2569.

Ritt, J.T., Andermann, M.L., and Moore, C.I. (2008). Embodied information processing: vibrissa mechanics and texture features shape micromotions in actively sensing rats. Neuron *57*, 599–613.

Sachdev, R.N., Sellien, H., and Ebner, F. (2001). Temporal organization of multi-whisker contact in rats. Somatosens. Mot. Res. *18*, 91–100.

Schmahmann, J.D. (2003). Vascular syndromes of the thalamus. Stroke *34*, 2264–2278.

Schwarz, C., Hentschke, H., Butovas, S., Haiss, F., Stüttgen, M.C., Gerdjikov, T.V., Bergner, C.G., and Waiblinger, C. (2010). The head-fixed behaving rat–procedures and pitfalls. Somatosens. Mot. Res. *27*, 131–148.

Shapley, R., and Victor, J.D. (1979). The contrast gain control of the cat retina. Vision Res. *19*, 431–434.

Sharpee, T.O., Sugihara, H., Kurgansky, A.V., Rebrik, S.P., Stryker, M.P., and Miller, K.D. (2006). Adaptive filtering enhances information transmission in visual cortex. Nature *439*, 936–942.

Sherman, S.M. (1996). Dual response modes in lateral geniculate neurons: mechanisms and functions. Vis. Neurosci. *13*, 205–213.

Sherman, S.M. (2001). A wake-up call from the thalamus. Nat. Neurosci. *4*, 344–346.

Steriade, M., McCormick, D.A., and Sejnowski, T.J. (1993). Thalamocortical oscillations in the sleeping and aroused brain. Science *262*, 679–685.

Stüttgen, M.C., Rüter, J., and Schwarz, C. (2006). Two psychophysical channels of whisker deflection in rats align with two neuronal classes of primary afferents. J. Neurosci. *26*, 7933–7941.

Suzuki, S., and Rogawski, M.A. (1989). T-type calcium channels mediate the transition between tonic and phasic firing in thalamic neurons. Proc. Natl. Acad. Sci. USA *86*, 7228–7232.

Swadlow, H.A., and Gusev, A.G. (2001). The impact of 'bursting' thalamic impulses at a neocortical synapse. Nat. Neurosci. *4*, 402–408.

Temereanca, S., Brown, E.N.N., and Simons, D.J. (2008). Rapid changes in thalamic firing synchrony during repetitive whisker stimulation. J. Neurosci. *28*, 11153–11164.

Van der Werf, Y.D., Witter, M.P., Uylings, H.B.M., and Jolles, J. (2000). Neuropsychology of infarctions in the thalamus: a review. Neuropsychologia *38*, 613–627.

Varela, C. (2014). Thalamic neuromodulation and its implications for executive networks. Front. Neural Circuits *8*, 69.

Waiblinger, C., Brugger, D., Whitmire, C.J., Stanley, G.B., and Schwarz, C. (2015a). Support for the slip hypothesis from whisker-related tactile perception of rats in a noisy environment. Front. Integr. Nuerosci. *9*, 53.

Waiblinger, C., Brugger, D., and Schwarz, C. (2015b). Vibrotactile discrimination in the rat whisker system is based on neuronal coding of instantaneous kinematic cues. Cereb. Cortex *25*, 1093–1106.

Wang, X., Wei, Y., Vaingankar, V., Wang, Q., Koepsell, K., Sommer, F.T., and Hirsch, J.A. (2007). Feedforward excitation and inhibition evoke dual modes of firing in the cat's visual thalamus during naturalistic viewing. Neuron *55*, 465–478.

Wang, Q., Webber, R.M., and Stanley, G.B. (2010). Thalamic synchrony and the adaptive gating of information flow to cortex. Nat. Neurosci. *13*, 1534–1541.

Wark, B., Lundstrom, B.N., and Fairhall, A. (2007). Sensory adaptation. Curr. Opin. Neurobiol. *17*, 423–429.

Wolfart, J., Debay, D., Le Masson, G., Destexhe, A., and Bal, T. (2005). Synaptic background activity controls spike transfer from thalamus to cortex. Nat. Neurosci. *8*, 1760–1767.

Wolfe, J., Hill, D.N., Pahlavan, S., Drew, P.J., Kleinfeld, D., and Feldman, D.E. (2008). Texture coding in the rat whisker system: slip-stick versus differential resonance. PLoS Biol. *6*, e215.

Zagha, E., Casale, A.E., Sachdev, R.N.S., McGinley, M.J., and McCormick, D.A. (2013). Motor cortex feedback influences sensory processing by modulating network state. Neuron *79*, 567–578.

Zheng, H.J.V., Wang, Q., and Stanley, G.B. (2015). Adaptive shaping of cortical response selectivity in the vibrissa pathway. J. Neurophysiol. *113*, 3850–3865.